Periodica Polytechnica Civil Engineering

62(2), pp. 323–329, 2018
https://doi.org/10.3311/PPci.11253

RESEARCH ARTICLE

Monitoring of Excessive Deformation of Steel Structure Extra-High Voltage Pylons

Lačezar Ličev[1*], Jakub Hendrych[1], Jan Tomeček[1], Radim Čajka[2], Martin Krejsa[3]

Received 12 July 2017; Revised 21 September 2017; Accepted 04 October 2017

Abstract

Reliability and security of a power transmission depends on the state of the power grid and mainly on the state of the Extra-High Voltage pylons. The paper deals with deformation analysis of existing steel structure of selected Extra-High Voltage pylons which showed excessive differences comparing to the original design. In the assessment of the situation, geodetic survey of selected pylons of power grid that showed the greatest deformation was performed. On taken images, deformation of steel structures by using the FOTOMNG system was also analyzed. The proposed method allows a modeling of the structure of the object based on precisely obtained photographic documentation of the current state. It also represents a very effective method which allows to quickly and efficiently analyze the deformation in the structure of Extra-High Voltage pylons in the critical position of the power grid. Other benefits include the possibility of repeatable and safe measurement.

Keywords

geodetic survey, FOTOM, image processing, radon transform, perspective transform, digital photogrammetry

1 Department of Computer Science,
Faculty of Electrical Engineering and Computer Science,
VŠB – Technical University of Ostrava,
17. listopadu 15, Ostrava-Poruba 708 33, Czech Republic
2 Department of Structures,
Faculty of Civil Engineering,
VŠB – Technical University of Ostrava,
Ludvíka Podéště 17, Ostrava-Poruba 708 33, Czech Republic
3 Department of Structural Mechanics,
Faculty of Civil Engineering,
VŠB – Technical University of Ostrava,
Ludvíka Podéště 17, Ostrava-Poruba 708 33, Czech Republic
* Corresponding author, email: lacezar.licev@vsb.cz

1 Introduction

In the context of scientific research and expert activities at the Faculty of Civil Engineering, VŠB-TU Ostrava was performed static analysis of deformed steel structure of selected Extra-High Voltage pylons which clearly showed excessive differences to the original design in the horizontal direction. With static assessment of the situation was performed correctness analysis of design. Emphasis was placed on:

- assessment of the interaction of the base structure and subsoil [1, 2, 16] and checking the correctness of the base structure design, focusing on the depth of the base structure, observance of technological progress in the construction, design of shape base structure, design of support and design of concrete classes [3],
- checking the correct determination of extreme loads [13] - horizontal strokes in conductors, horizontal strokes in conductors, which are supported by assessed pylons with regard to the prescribed height of conductors above ground and prescribed values of deflections at certain temperatures,
- background checks of support system [4, 5] using mathematical modelling [6, 7] and checking the correctness of design of steel structures pylons, with a focus on the analysis of extreme load effects caused by its own weight of conductors and strokes in conductors,
- verifying the correctness of the construction process, used technologies and materials with respect to local conditions, climatic influences and deviations that cannot be overlooked during realization [14, 15, 17, 18, 19, 20, 21].

Steel pylons are designed for dual lines 2 × 110 kV. The steel structure is made of steel S355J2. The pylons are made of three parts, which are installed together one by one and firmly fixed together with steel pins.

Pylon structure is situated on the pylon base of concrete class C30/37. Base plate thickness of 400 mm is reinforced by KARI nets 8/150-8/150 mm and pylon base is reinforced by rods of diameter 16 mm.

In the analysis of excessive horizontal deformation of steel pylons were first performed geodetic surveying of actual deformations.

The geodetic measurement of semi-height and altitude of the column's verticality and the flatness of the concrete footing were carried out in selected, perpendicular, directions to the reflecting labels placed on the centre of the columns. Geodetic measurements were performed by the total station TOPCON OS–103, Art.No.CT0703 with three times the distance measurement. The total station was set to the most accurate distance measurement mode. The difference in length measurement did not exceed 1 mm.

The measurements were made in the local position and height system for each column separately. Simultaneously with the measurement of the column verticality, the height of the concrete footings was measured repeatedly from two positions.

The resulting deviations of the columns centre from the vertical axis were determined from two independent measured values - from the angular and longitudinal values in the given direction and the longitudinal values in the perpendicular direction. The difference of the independent measurements with applied calculations did not exceed a deviation of 3 mm. The resulting values were processed into a separate protocol for each column separately, indicating vertical positional deviations, height-targeted locations (measurement targets) and elevation differences of the top of the concrete footing.

Measurement was focused particularly on the pylons situated in the corners of power grid, which showed the greatest deformations. Planimetric and altimetric focus of pylon verticality and flatness of the concrete base were carried out in selected, perpendicular directions, by using of reflective labels. First one was placed in height of the base structure, other two on the contacts of pylon parts and last one on the top of each measuring mast always in its axis. Simultaneously with the measurement of verticality of pylons was also repeatedly targeted the elevation of the concrete base from two positions. The actual measured values of deformation of pylons were an important basis for the assessment of serviceability limit state of analysed pylons.

Alternatively, based on the given images of the support system of steel pylons, was performed evaluation of geometry of deformed steel pylons by FOTOM^{NG} computing system [8–10, 12].

2 Evaluation of the pylon from a single image

Before performing of the actual evaluation of the Extra-High voltage pylons from a single image, we must follow a few rules and actions, such as the transformation of the image and image rotation, more in sections 2.1, 2.2 and 2.3.

2.1 Image transformation of Extra-High Voltage pylons

To evaluate the status of the pylon from a single image we must follow these rules:

- The axis of the camera must aim towards the centre of observed pylon.
- Rotating the image to remove the effects of tilt caused by diversion of base structure, see section 2.2.
- The axis of the camera must be perpendicular to the plane of the pylon in the direction of tilt, see section 2.3.

2.2 Image rotation by definition of own two points

The whole process of calculation is dependent on the definition of two control points on the image. After selecting this function, listener is added to the image component that responds to mouse clicks. We distinguish whether it is a first clicks (i.e. the definition of the first control point) or the second click (i.e. definition of the second control point). The coordinates of the two points $A[x_1, y_1]$ and $B[x_2, y_2]$, are saved.

Now is executed the calculation algorithm. At the beginning both vectors are calculated (1). Thus, the vector $\vec{v} = (v_1, v_2)$, which is represented by two control points (A, B) and the vector $\vec{u} = (u_1, u_2)$, which represents the perpendicular vector. Each of the coordinates in $\vec{v}$, $\vec{u}$ are calculated as the difference of x-coordinates and difference of y-coordinates of both control points. From vectors $\vec{v}$ and $\vec{u}$ is subsequently calculated angle of two vectors in radians (2). Value in radians is additionally converted into angular units (3). Apply this angle to rotate the image would not be ideal, because it was necessary to additionally determine the direction of the rotation – if the angle is negative or positive. Direction of rotation is determined from the coordinates $[x_1, y_1]$ and $[x_2, y_2]$ of control points by comparing x-coordinates and y-coordinates of both points.

$$\begin{aligned} v_1 &= x_2 - x_1, \\ v_2 &= y_2 - y_1, \\ u_1 &= x_2 - x_1, \\ u_2 &= y_2 - y_1, \end{aligned} \tag{1}$$

$$a = \frac{u_1 v_1 + u_2 v_2}{\sqrt{u_1^2 + u_2^2} \cdot \sqrt{v_1^2 + v_2^2}} \tag{2}$$

$$\alpha = \frac{\cos^{-1} a \cdot 180}{\pi} \tag{3}$$

Now there is a possibility to apply the rotation angle on the image. To rotation of each pixel are used Eq. (4) expressed from a transformation matrix for rotation [9, 10]. These equations were modified for calculating with the image centre point $S[S_x, S_y]$ around which will rotate individual pixels. We get from the original pixel coordinates x, y new pixel coordinates n_x, n_y rotated by an angle α. Image rotation in FOTOM^{NG} system is realized as a separate module.

$$\begin{aligned} n_x &= \left(x - S_x\right) \cdot \cos\alpha - \left(y - S_y\right) \cdot \sin\alpha + S_x, \\ n_y &= \left(x - S_x\right) \cdot \sin\alpha + \left(y - S_y\right) \cdot \cos\alpha + S_x \end{aligned} \tag{4}$$

2.3 Tilt of image by using perspective transformation

This new functionality in FOTOM^{NG} system provides tilting of image in the Z axis against to an observer in the interval <–90°, 90°>. Reason of this implementation was to eliminate distortion caused by capturing of individual images, e.g. in the case of photographing the Extra-High Voltage pylons. In the best scenario, the axis of scanning device (camera) should be perpendicular to the observed object. However, if we scanned high objects we have to place a camera at large distance from the observed object - decreasing the accuracy of the measurement of the image. Therefore we commonly used closer distances for scanning object, but with a tilt of scanning device. However this leads to distortion because top of the Extra-High Voltage pylon will appear smaller due to the large height and distance from the viewer than the lower part of the pylons, which is closer to the observer. Here we can observe the perspective distortion. It may be removed by using perspective transformation - allowing us to tilt the image so that it is perpendicular to the axis of scanning device. The upper part of the final image will be expanded and the lower part will be narrowed (assuming that the image is tilted toward the observer).

$$\begin{bmatrix} x' \\ y' \\ w \end{bmatrix} = \begin{bmatrix} m_{00} & m_{01} & m_{02} \\ m_{10} & m_{11} & m_{12} \\ m_{20} & m_{21} & m_{22} \end{bmatrix} \cdot \begin{bmatrix} x \\ y \\ 1 \end{bmatrix} = \begin{bmatrix} m_{00}x & m_{01}y & m_{02} \\ m_{10}x & m_{11}y & m_{12} \\ m_{20}x & m_{21}y & m_{22} \end{bmatrix} \quad (5)$$

where m_{ij} are the matrix variables realizing the transformation; x, y are source coordinates and x', y' are homogeneous coordinates of the target destination.

$$x' = \frac{m_{00}x + m_{01}y + m_{02}}{m_{20}x + m_{21}y + m_{22}}, \qquad y' = \frac{m_{10}x + m_{11}y + m_{12}}{m_{20}x + m_{21}y + m_{22}}, \quad (6)$$

where m_{ij} are the matrix variables realizing the transformation; x, y are source coordinates and x', y' are inhomogeneous coordinates of the target destination. When using this function, the user has ability to set an interval <–90°, 90°> by slider component. Both limit values, gets image into a horizontal position to an observer, so it cannot be seen. The actual understanding and implementation of perspective transformation requires additional study, but the FOTOM^{NG} system uses JAI (Java Advanced Imaging) library, that implements a classes for perspective transformation. Perspective transformation is represented by using a 3 × 3 matrix (5), which will transform the homogeneous sources coordinates (x, y, 1) into a target destination with coordinates (x', y', w). If desired, the recovery of inhomogeneous coordinates, we must divide x' and y' by w (6). The only problem was the application of the tilt angle into this method, which was resolved by deploying scale. This scale allows the correct tilt angle in the interval <–90°, 90°> based on the image size and direct proportion. At Figure 2 we can see the tilt angle that is applied to the image. Tilt of image in FOTOM^{NG} system is realized as a separate module. Figure 1 shows the image after tilting.

Fig. 1 Tilt of image by using perspective transformation (pylon 13).

Tilting the image is also expanded with own tilt angle calculation. For this algorithm are important two parameters. The first is the size of the object that is measured h and the second is the camera distance from the object base. Based on these values, we can use trigonometric functions (7) to calculate the angle α, which forms the axis of view (towards the centre of the observed object) and the line connecting point of the observer and the base point of the observed object.

The whole situation is shown in Figure 2, where the parameters we use are: Object height is 28 meters and distance between the object and the camera is 60 meters.

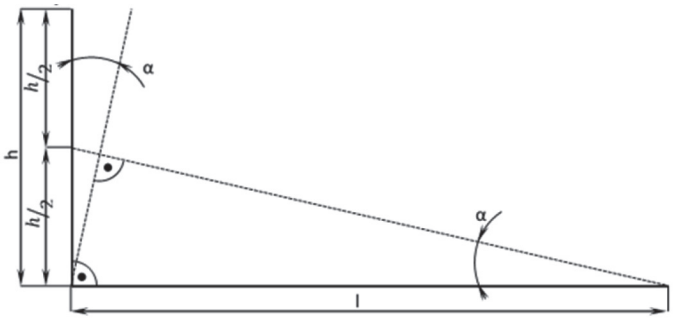

Fig. 2 Drawing evaluate the tilt angle.

Where h is the size of the observed object, l is the distance between camera and the object base and α is the tilt angle of the image, which we can compute as:

$$\tan\alpha = \frac{\frac{h}{2}}{l} \tag{7}$$

3 Evaluation of the pylon status by using of image series

3.1 The principle of the radon transform

Radon transform means the integral transformation of continuous [11], in this case the image function $f(x,y)$. The main idea of radon transform is based on the fact that the observed object can be fully reconstructed from a set of projections of the same scene, which contains this object. By the term of projection is meant a set of infinitely narrow focused ray projections acquired at one angle shooting. Attenuation of a single ray R_τ obtained under angle θ_0 can be expressed as:

$$p_{\theta_0} = \int_{R_\tau} f(x,y)\,\mathrm{d}r. \tag{8}$$

The variable r is defined as the path of the light ray. For any ray and angle of shooting a scene we can express the radon transform as:

$$p(\tau,\theta) = \int_{-\infty}^{\infty}\int_{-\infty}^{\infty} f(x,y)\,\delta(x\cos\theta + y\sin\theta - t)\,\mathrm{d}x\mathrm{d}y \tag{9}$$

where δ indicates the Dirac delta function.

The newly formed space $\mathrm{p} \subset \mathbb{R}^2$, representing the set of projections is called a sinogram. It is clear that the Eq. (9) is periodic to angles θ with period 2π.

However, since the range of calculations is situated in the visible spectrum of electromagnetic radiation, it is necessary to introduce several assumptions and simplifications. First, the character of the images provides simplification based on the assumption that rays are moving by the shortest path to the detector (camera), and thus prevents the occurrence of refraction. Next, since everything, except the observed object, can be considered as fully transparent and conversely the observed pylon as a source of hundred-percent attenuation we can introduce the assumption that $p_\theta \in \{0; 255\}$. It means that also the final sinogram will have only two values of brightness.

3.1.1 Filtered back projection

This is a reconstruction algorithm that from the known sinogram searches for the original image with the object by using the inverse radon transform.

$$f(x,y) = \int_0^{2\pi} g_\theta(x\cos\theta + y\cos\theta)\,\mathrm{d}\theta, \tag{10}$$

where

$$g_\theta = \mathcal{F}^{-1}(HP \cdot \mathcal{F}(p_\theta)), \tag{11}$$

where $\mathcal{F}$ and $\mathcal{F}^{-1}$ indicates the Fourier transformation operator respectively inverse transformation. HP is one-dimensional and high-pass "ramp" filter in the frequency domain. The aim of this filter is to minimize the star artefact that is caused by an insufficient number of projections and thus this filter is increasing the SNR (Signal to Noise Ratio). The advantage of this reconstruction method is especially low computational complexity. However, it is necessary to have a sufficient number of projections.

The newly designed module for the FOTOM^{NG} system allow to making cuts on selected images and then perform for each cut inverse radon transform (back projection). Cuts can be edited by user, determine their location or quantity. After performing an inverse radon transform module creates an image of the reconstructed object on the current cut along with the star artefact and an image of the reconstructed object without the star artefact.

To be able to identify an object of interest on each image (Extra-High Voltage pylon) and perform cuts, it is necessary to do some preparations in the form of several steps. The first step is to define the area of the image where the object is located. Demarcation of the area is intended for all the images of the observed object. Realized module allows the user to specify an area where will be the object detected. The selection is then applied to all images. Here we can encounter with the problem of unwanted objects in the images that are not the object of interest and their reconstruction is not required. In the specific case of images of Extra-High Voltage pylon some individual images contain distant objects, such as trees in the background or other objects of surrounding landscape. This problem is solved by means of image operations such as edge detection and thresholding. In spite of application of both methods we can still encounter problems of incomplete lines (edges) of the pylon, which can lead to problems when we perform cuts. This problem arises with unfavourable lighting conditions when the images are created. The image contains different brightness values and the line of the pylon blend into the background or other objects. This problem can be solved by using existing tools in the FOTOM^{NG} system – user painted contour lines.

3.2 Implementation of the module and measurement

The images of Extra-High Voltage pylons were taken by workers of the Faculty of Civil Engineering, VŠB-TU Ostrava and simultaneously re-measured by using standard surveying techniques used in practice. When taking a photo we used constant distance of 60 meters between camera and observed object. Pylon was scanned from an initial angle of 0° up to the final angle of 360°, with 45° stepping. The result contained 8 images.

To be able to reconstruct the selected pylon and perform subsequent measurement, FOTOM^{NG} system was expanded with new module. Designed module allows us to perform cuts, which can be edited by user, determine their location or quantity. After performing an inverse radon transform module creates an image of the reconstructed object on the current cut along with the star artefact (Figure 3) and an image of the reconstructed object without the star artefact (Figure 4).

Fig. 3 Reconstructed object with the star artefact.

Fig. 4 Reconstructed object without the star artefact.

After performing five cuts on pylon and applying an inverse radon transform was created five reconstructed objects in five selected places on the pylon. Subsequently the individual images of reconstructed objects were used as input for 3D modelling of objects and their measurements.

3.3 Image pre-processing

For images of the Extra-High Voltage pylon was necessary to apply multiple image pre-processing operations [9, 10], which allowed the correct reconstruction of the desired object by using the inverse radon transform [11]. These operations are: edge detection and binary thresholding binary that manipulate with images in shades of grey.

After application of the above mentioned operations the images meet the requirements of the inverse radon transform and can be successfully used as input data for the embedded module that implements the inverse radon transform.

4 Measurement of tilt of the pylon

4.1 The resulting deformation of Extra-High Voltage pylon

Given the nature of the support system of the steel pylons are the resulting deformation caused by:

- deformation (tilt) of pylon base structure,
- rotation of the pylon in two assembly joints,
- bending of the conductor's tension effects in three parts of the each pylon.

These three deformations were evident on the first inspection of existing structure, but also in the analysis of geodetic measurements on the most deformed pylons.

The assessment of the serviceability limit state based on a comparison of the values actually measured deformations on the pylons (steel structure deformation w_{real} and rotation of pylon base structure w_{pbs}) with the values of allowable deflection at the top of the pylon, which indicates the valid standard. Actually measured values of the horizontal deflection of structure at most deformed pylons in the corners of the power grid were in ranged from 162 mm to 346 mm.

In the following text, are analysed the resulting deformation values of pylons obtained from the FOTOM^{NG} system.

4.2 Measurement results of deviation of the Extra-High Voltage pylons from a single image

Table 1 Measured deviation from a single image (number four), without the deviation of the concrete base.

Pylons	#6	#7	#13	#17
Deviation [mm]	222.22	-	172.6	326.16

A total of eight images were taken for the pylon #13. It was essential to find an image that corresponded with the direction of the geodetic survey – important for comparing both methodologies (more in section 5). To find such an image in the series, geodetic labels were used. These labels were attached during the geodetic survey on the pylon axis at three heights for the eastern and northern view. Ideal was an image number four (see Table 1 results), which corresponded to the eastern direction from geodetic survey.

It is important to add that the pylon #7 could not be measured, because there was not any image corresponding to the eastern view of geodetic survey. Therefore, the measurement cannot be compare.

4.3 Measurement results of deviation of the Extra-High Voltage pylons by using of radon transform

Table 2 Maximal measured deviation from image series, without the deviation of the concrete base.

Pylons	#6	#7	#13	#17
Max. deviation [mm]	303.0	-	309.89	485.94

This methodology has huge advantage against geodetic survey. We can acquire maximal deviation of the observed object (see Table 2). During the geodetic survey, the labels are attached according to the eastern or northern direction. But this not provides the maximal deviation, but only deviation for the current view.

Again, pylon #7 cannot be measured, because the image series has only 7 images.

Using of radon transform has another advantage. In our research we also create 3D voxel model of measured Extra-High Voltage pylons from 100 cuts (see Figure 5).

Fig. 5 3D voxel model of Extra-High Voltage pylon #3.

4.4 The accuracy of the measurement

Overall measurement accuracy depends on several factors:

1. Resolution of captured images – non-compliance leads to poor pixel/metric unit ratio. Therefore, for both types of measurements (section 4.2 and 4.3) in the FOTOMNG system, the 1px deviation is approximately 28 mm.
2. Compliance with the conditions for capturing the images – non-compliance leads to the failure of eliminating the perspective distortion and following radon transformation. Next the deviation distortion due to the camera non-horizontal position during the capturing.

In the case of the first point, the only solution is to take high-resolution images. In general, the higher resolution of the image leads to the better accuracy of the measurement.

In the case of the second point, we can use the software editing directly on the FOTOM^{NG} system. For example – non-horizontal position of the camera can be corrected by rotation of the image.

5 Evaluation of results achieved

Four high-voltage pylons were evaluated using two methods - using geodetic survey (see Figure 6) and system FOTOM^{NG}.

When geodetic measurements and photographing of pylons were observed following procedure – planimetric and altimetric focus of pylons verticality and flatness of the concrete footings were performed at selected, orthogonal directions. Focus of the pylons was done using a total station, which was set up to the most accurate mode of distance measurement. The difference of repeated measurements of lengths did not exceed 1 mm. All measurements were focused on local horizontal and vertical system of each pylon separately. Along with measuring of pylons verticality was also aimed elevation of the concrete footings and repeatedly from two standpoints. The resulting deviations from the centre of the pylons in vertical axis were determined from two independent measured values (from angle and distance values in a given direction and from distance values in the perpendicular direction). Unlike these calculated independent measurements, the deviation does not exceed 3 mm. In the course geodetic survey was carried out photographing of pylons in accordance with the agreed terms. The thus obtained images were used in a system FOTOM^{NG}.

Results obtained from geodetic measurements on the existing structures of the four Extra-High Voltage pylons exhibit sufficient match with the values of the horizontal deformations, arising from the numerical analysis of FOTOM^{NG} system (see Table 3).

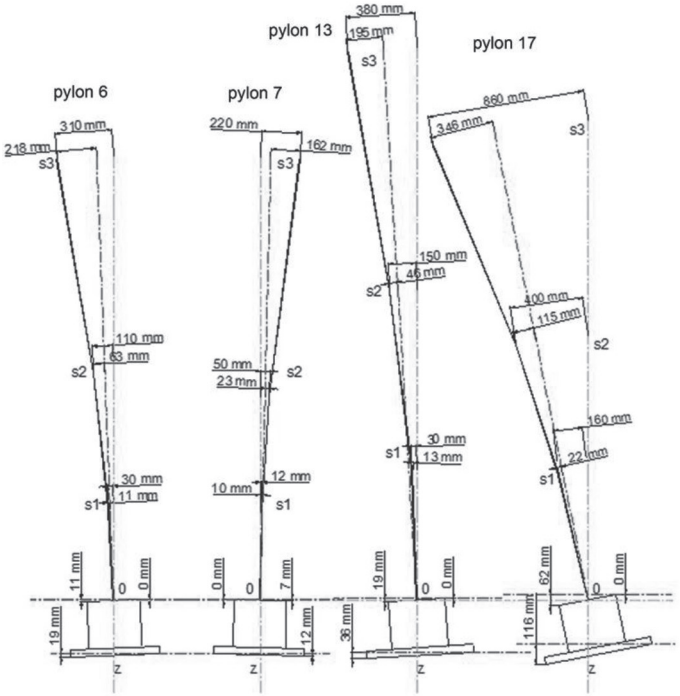

Fig. 6 Graphical representation of the geodetic measured deformations of pylons 6, 7, 13 and 17.

The inaccuracies against the geodetic measurement can be justified by the quality of submitted images. Photos of observed structure of Extra-High Voltage pylons were taken at positions with constant distance of l = 60 m, but it was not possible, given the nature of the terrain, to keep their same height. In spite of this lack is precision of obtained horizontal deviations from the vertical pylon sufficient for the practical purposes.

Table 3 The difference between the two methodologies.

Pylons	#6	#7	#13	#17
Dev. FOTOM^{NG} system [mm]	222.22	-	172.6	326.16
Dev. geodetic survey [mm]	218	162	195	346
Difference [mm]	4.22	-	22.4	19.84

6 Conclusions

In this paper we dealt with deformation analysis of existing steel structure of selected Extra-High Voltage pylons. Analysis of the deformation state was performed based on geodetic measurements, but also by using the FOTOM^{NG} system, which was theoretically described in detail. Comparison was made between deformation values, which have been obtained by using both approaches, and was achieved the satisfactory compliance. The differences in the results from both methodologies can be caused by non-compliance of the conditions during the capturing individual images – the constant distance between observed object and camera position, the direction of the camera axis to the centre of the observed object, stepping between individual images (the same angle) and the horizontal position of the camera during the capturing. However, most of the conditions are difficult to keep, because of difficult terrain.

Despite the small inaccuracies, the results are very positive. The FOTOM^{NG} system was differed from 4 to 22 mm, which is negligible in relation to the height of the observed object (30.2 meters). Next time, if all conditions will meet, accuracy will increase significantly. Even though pylon #7 has not been measured, we estimate the results (based on the other measurements) within the above mentioned range.

The measurement methodology itself in the FOTOM^{NG} system brings clear benefits – speed, efficiency, repeatability of the measurement and safety. A great advantage is the use of radon transformation to obtain maximum deviation and providing a 3D voxel model.

The described method of numerical modelling of construction object based on precisely obtained photo documentation of current state represents a very effective way to quickly and efficiently analyse the deformation state of structures.

Acknowledgement

The paper has been partially supported by Grant of SGS No. SP2015/142 and also has been completed thanks to the financial support provided to VSB-Technical University of Ostrava by the Czech Ministry of Education, Youth and Sports from the budget for conceptual development of science, research and innovations for the 2017 year.

References

[1] Čajka, R., Matečková, P., Januliková, M., Stará, M. "Modelling of Foundation Structures with Slide Joints of Temperature Dependant Characteristics". In: Proceedings of the Thirteenth International Conference on Civil, Structural and Environmental Engineering Computing, Chania, Crete; Greece; 6–9 September 2011. Code 89029. p. 10.

[2] Čajka, R. "Soil-structure interaction in case of exceptional mining and flood actions". In: Improvement of Buildings' Structural Quality by New Technologies: Proceedings of the Final Conference of COST Action C12, 20–22 January 2005. Innsbruck, Austria, pp. 369–376. CRC Press, 2005.

[3] Kralik, J., Jendzelovsky, N. "Contact problem of reinforced-concrete girder and nonlinear Winkler foundation". In: International Conference Geomechanics 93, Strata Mechanics/Numerical Methods/Water Jet Cutting/Mechanical Rock Disintegration, pp. 233–236. 1993.

[4] Cajka, R., Krejsa, M. "Validating a computational model of a rooflight steel structure by means of a load test". *Applied Mechanics and Materials*, 501–504, pp. 592–598. 2014. https://doi.org/10.4028/www.scientific.net/AMM.501-504.592

[5] Major, M., Kulinski, K. "Comparative Numerical Analysis Of Advertising Board Tower Using Adina And Autodesk Robot Structural Analysis". *Transactions of the VŠB – Technical University of Ostrava, Civil Engineering Series*, 15(2), p. 10. 2016. https://doi.org/10.1515/tvsb-2015-0015

[6] Flodr, J., Krejsa, M., Mikolasek, D., Sucharda, O., Zidek, L. "Mathematical modelling of thin-walled cold-rolled cross-section". *Applied Mechanics and Materials*, 617, pp. 171–174. 2014. https://doi.org/10.4028/www.scientific.net/AMM.617.171.

[7] Krejsa, M. "Probabilistic failure analysis of steel structures exposed to fatigue". *Key Engineering Materials*, 577–578, pp. 101–104. 2014. https://doi.org/10.4028/www.scientific.net/KEM.577-578.101

[8] Žára, J., Beneš, B., Felkel, P. "*Moderní počítačová grafika*". Vyd. 1. p. 448. Computer Press, Praha. 1998. (in Czech).

[9] Ličev, L. "Analýza, modelování, rozpoznávání a vizualizace procesu měření objektů na snímcích". p. 125. Computer Press, Brno. 2010. (in Czech).

[10] Ličev, L. "Systém FOTOMNG, architektura, funkce a použití". p. 230. BEN Praha, 2015. (in Czech).

[11] Ptáček, J. "Filtrovaná zpětná projekce – rozšířený popis, Univerzita Palackého v Olomouci". 2013.

[12] Lichev, L., Tomechek, J., Hendrych, J., Cajka, R., Krejsa, M. "New methods of evaluation of deformation structure extra-high voltage pylons". In: *15th International Multidisciplinary Scientific Geoconference and EXPO - SGEM 2015*, Albena, Bulgaria. Vol. 1, Issue 2, pp. 215–224. 2015. https://doi.org/10.5593/SGEM2015/B21/S7.028

[13] Kotrasova, K., Grajciar, I., Kormaníkova, E. "Dynamic time-history response of cylindrical tank considering fluid - Structure interaction due to earthquake". *Applied Mechanics and Materials*, 617, pp. 66–69. 2014. https://doi.org/10.4028/www.scientific.net/AMM.617.66.

[14] Kala, Z. "Sensitivity analysis in advanced building industry". *Procedia - Social and Behavioral Sciences*, 2(6), pp. 7682–7683. 2010. https://doi.org/10.1016/j.sbspro.2010.05.177

[15] Protivinsky, J., Krejsa, M. "Material study of a short seismic link in a dissipative structure of a vertical industrial boiler". *Applied Mechanics and Materials*, 623, pp. 10–17. 2014. https://doi.org/10.4028/www.scientific.net/AMM.623.10

[16] Cajka, R. "Accuracy of Stress Analysis Using Numerical Integration of Elastic Half-Space". *Applied Mechanics and Materials*, 300–301, pp. 1127–1135. 2013. https://doi.org/10.4028/www.scientific.net/AMM.300-301.1127

[17] Cajka, R. "Analysis of Prestressed Concrete Tower for Wind Turbine Generator". *Advanced Materials Research*, 772, pp 622–629. 2013. https://doi.org/10.4028/www.scientific.net/AMR.772.622

[18] Jiang, L., Xu, X., Di, Z. "Research on contact characteristics of the foundation for wind turbine generator system". *Applied Mechanics and Materials,* 63–64, pp. 633–636. 2011. https://doi.org/10.4028/www.scientific.net/AMM.63-64.633

[19] Szafran, J. "An experimental investigation into failure mechanism of a full-scale 40 m high steel telecommunication tower". *Engineering Failure Analysis*, 54, pp. 131–145. 2015. https://doi.org/10.1016/j.engfailanal.2015.04.017

[20] Edyta, P., Rajmund, O. "Measurements of deformations of inner structures of multi-flue industrial chimneys". *International Multidisciplinary Scientific GeoConference Surveying Geology and Mining Ecology Management, SGEM,* 2, pp. 317–324. 2013.

[21] Xie, Q., Sun, L. "Experimental study on the mechanical behavior and failure mechanism of a latticed steel transmission tower". *Journal of Structural Engineering (United States),* 139 (6), pp. 1009–1018. 2013. https://doi.org/10.1061/(ASCE)ST.1943-541X.0000722